

D4.1 Multiscale numerical model

Project acronym: **THROMBUS**,

Project full title: A quantitative model of thrombosis in intracranial aneurysms

- Instrument type: Collaborative Project
- Project coordinator: CNRS

- Contract nr.: FP7-ICT-2009-6- 269966
- Start date: Feb 1, 2011
- Duration: 36 months

Report identification

Period from: 01/02/2011
 To: 30/01/2012
 Due date of report: M12
 Actual submission date: M12
 Revision: [final]

Dissemination level:

CO – Confidential. Only for members of the consortium (including the Commission services)

PU

Partners involved

Author of this report	Bastien Chopard	UNIGE
Contributors involved in the reported work (from same organisation or others)	Orestis Malaspinas, Rafik Ouared	UNIGE
	Eric Lorenz, Lampros Mountrakis, Alfons Hoekstra	UvA
	Simon Zimny, Joerg Bernsdorf	GRS



D4.1 Multiscale numerical model

Project acronym: *THROMBUS*

Project full title: A quantitative model of thrombosis in
intracranial aneurysms

Grant agreement no.: 269966

Due-Date:	M12
Delivery:	M12
Lead Partner:	UNIGE
Dissemination Level:	PU
Status:	Final
Approved:	
Version:	1.2

DOCUMENT INFO

Date and version number	Author	Details
7-01-2012 v0.1	B. Chopard (UNIGE)	document structure
17-01-2012 v0.2	Simon Zimny (GRS)	Contributions
17-01-2012 v0.2	Eric Lorenz (UvA)	Contributions
17-01-2012 v0.2	Orestis Malaspinas (UNIGE)	Contributions
17-01-2012 v0.2	Rafik Ouared (UNIGE)	Contributions
25-01-2012 v.02	Orestis Malaspinas (UNIGE)	corrections
25-01-2012 v.03	B.Chopard (UNIGE)	integration
27-01-2012 v.03	Eric Lorenz (UvA)	corrections
29-01-2012 v.1	B.Chopard (UNIGE)	integration
31-01-2012 v.1	A Hoekstra (UvA)	corrections
29-01-2012 v.1.1	B.Chopard (UNIGE)	Finalization
17-02-2012 v.1.2	G. Courbebaisse (INSA-Lyon)	Reviewing

TABLE OF CONTENTS

Executive summary	5
1 Introduction	7
2 Results	7
2.1 The macroscopic numerical model.....	8
2.1.1 The Palabos software	9
2.1.2 Particle transport model	10
2.1.3 The discrete particle method	12
2.1.4 Boundary conditions	13
2.1.5 The lattice Boltzmann advection-diffusion method . .	14
2.1.6 Boundary conditions	15
2.1.7 Advantages and drawbacks of each model	15
2.1.8 Thrombosis formation model	15
2.1.9 Simulation	16
2.1.10 Cellular automaton transport model	19
2.1.11 LB Advection-diffusion model	20
2.2 The microscopic numerical model	21
2.2.1 Hierarchical model of blood flow	21
2.2.2 Preliminary Model of RBCs and Platelets Suspended in Flow	23
2.2.3 Simulations	26
2.3 Multiscale description of thrombosis	28
2.3.1 The Biological Processes	28
2.3.2 The Coupling Scheme	30
3 Conclusions.....	31
References	33

List of Tables

1 The parameters chosen for the spontaneous thrombosis present in this section, in lattice units.....	18
---	----

List of Figures

1	Comparison of the wall shear stress between Palabos and the commercial software CFX.	9
2	Simulation of the flow in a stented aneurysms, from a geometry and stent deployment provided by subcontractor StrokeLab.	10
3	Speedup of an aneurysm simulation performed on the CAD-MOS Bluegene/P. An efficiency of about 70% is obtained in the “strong” scaling case and on a span of two orders of magnitude in the number of processors.	11
4	The velocity norm in an aneurysm geometry from different angles (red for high velocity and blue for low).	11
5	Velocity and probabilities of being streamed along one principal axis. The overall probability of being advected along a vector c_i is made of the probabilities of being advected or not advected in each one of these principal axes.	12
6	Particle concentration (red for high concentration, blue for low) in the aneurysm viewed from two different axes when using the LB advection diffusion algorithm.	14
7	Probability of adhesion p_a with respect to the wall shear stress w_{ss} . The higher the w_{ss} the lower the probability of adhesion.	17
8	A patient specific geometry (with two different view angles) of the aneurysm used in this section to illustrate the macroscopic numerical model of thrombosis.	17
9	The scale separation map of the particles (and thrombus) and of the fluid flow. One can see that while the spatial scales are similar the temporal scales differ of many orders of magnitude.	18
10	The time evolution of the wall of the blood vessel (from left to right). As can be seen the aneurysm is disappearing with time. It can be noticed, that a part of the aneurysm lumen does not disappear completely, but is detached from the parents vessel. This unrealistic effect is a consequence of a too small diffusivity of the platelets.	19

11	The time evolution of the wall of the blood vessel (from left to right). As can be seen the aneurysm is being occluded as time goes on.	20
12	Illustration of the thrombus formation (black region) in a high resolution simulation.	21
13	HMM coupling between a macroscopic and a microscopic solver of the dynamics of a simple complex fluid (a monodisperse hard-sphere suspension here). Left: Scale Separation Map illustrating the separation of microscopic and macroscopic processes. Right: On the macroscale solvers for the dynamics of the fluid and the solid phase span the whole domain but don't resolve the spatiotemporal details of the fluid's constituents. On each lattice node of the macroscopic solvers a microscale solver can be invoked to obtain transport properties and viscosities for given boundary conditions defined by macroscopic shear-rate and fluid/solid volume ratio.	22
14	Left: In the SuMO model RBC's and platelets are represented by an FE model of the membrane. Coupling to the fluid is realized using the immersed boundary method applied at the membrane points. Middle: The mechanical model consists of points that are connected by spring-and-damper elements between neighboring membrane points to realize stretch and compression of surface elements (red), spring-and-damper elements between next-nearest membrane points to represent membrane bending forces (blue), and normal forces are applied in order to conserve the internal volume (green). Right: A curvature dependent lubrication correction is applied between membrane points of different cells to capture the hydrodynamical interaction between membranes realistically.	26
15	Snapshot of the simulations, without stent and stented with high and low porosity	27
16	The Biological Processes	28
17	The Coagulation Cascade	29
18	The Coupling Scheme	30

Executive summary

The goal of WP4 is to develop a numerical model of thrombosis in cerebral aneurysm. The chosen approach is to start from the dynamical model previously developed by UNIGE [18, 4] and to extend it to 3D¹ with geometries obtained from medical images, and physiological flow conditions. As the project goes on, this model will be validated from biological experiments conducted in WP2 and clinical observation obtained in WP3.

This deliverable is a first report on task 4.1, which focuses on (1) the current version of the macroscopic numerical model (a 3D version of the earlier model ported on the Palabos software), and (2) a fully detailed, microscopic numerical model for the transport of red blood cells (RBC) and platelets. The last part of task 4.1, namely the formulation of a multiscale model of the thrombosis phenomena is briefly discussed here. The final version will be presented in deliverable D4.2, due at M18.

The present deliverable also elaborates our vision of the work to be done in WP4 and its articulation with other WP's.

The main results of this first year of WP4 are

- A running macroscopic numerical model implementing the thrombosis original model of [18, 4]. This model is fully parallel, and has been tested on one patient specific geometry, with a set of ad hoc parameter. The thrombus formation is shown in a qualitative way and CPU issues are discussed.
- Microscopic simulations of RBC and platelets in suspension, performed in a simplified 2D geometry of an aneurysm. The results show that the distribution and transport of RBC and platelets in the aneurysms cavity can be influenced by their shape.

These two models represent a multiscale approach to the simulation of thrombosis in cerebral aneurysms as they focus on different levels of the process. The macroscopic model will simulate long time evolution, over the scale of the full geometry, whereas the microscopic model will capture the basic biological processes that occur among platelets, RBC and the wall, as well as their interaction with the fluid. They will be a bridge with in-vitro

¹In the image processing community, this corresponds to a 4D model as it is 3D in space and 1D in time.

experiments and will offer ways to validate the assumptions made in the macroscopic model.

The contributors to this task are UNIGE, UvA and GRS.

1 Introduction

This deliverable is a first report, after 12 months, on Task 4.1: *Multiscale model for thrombosis*. A main objective of WP4 is to adapt the numerical model of thrombosis in cerebral aneurysms proposed in [18, 4] in order to simulate the bloodflow and the thrombosis model in patient specific aneurysms, with and without stent. This new version has been developed in the Palabos Lattice Boltzmann (LB) software environment [21] and offer what we call here a *macroscopic* model of thrombosis as it is aimed at simulating the evolution of the thrombus at the scale of the full aneurysm and for times as long as several weeks of month. This model includes a flow solver, an advection-diffusion model for the platelets and red blood cells and the growth of the clot which modifies the flow conditions.

In order to have a hierarchical multiscale approach, a *microscopic* numerical model has also been developed to complement the *macroscopic* model described above. This microscopic model provides a detailed description of the behavior of red blood cells (RBC) and platelet in suspensions in the plasma. The goal of this detailed model is to offer a way to calibrate and validate some of the assumptions made in the coarse grained macroscopic model, in particular for the transport of blood particles. It also provides a way to interpret, in a numerical context, the biological experiments conducted in WP2 and to link them to the macroscopic model.

A third goal of task 4.1 is to propose a multiscale description of the thrombus formation, and its interaction with the blood flow. This description is based on the CxA multiscale methodology developed by UvA and UNIGE (see for instance [11]), using the concepts of Scale Separation Map (SSM) and coupling templates. This description will be presented in deliverable D4.2, multiscale thrombosis model, due at M18. In the present deliverable, only the the general concepts are briefly presented, as work is still in progress.

2 Results

This section describes in detail the achievements of task 4.1, after 12 months. This task will continue for another 6 months. We divided this section in three parts, each corresponding to the three sub-tasks described

above, namely: (1) a dynamical 3D macroscopic numerical model on Palabos, (2) fully detailed suspension model, and (3) the multiscale formulation of thrombosis,

2.1 The macroscopic numerical model

The THROMBUS project aims at a better understanding of the physiological processes that induce the thrombosis in cerebral aneurysms in order to be able to understand the effect of a stents and to be able to optimize their shape to be as efficient as possible.

A part of this project is dedicated to the macroscale numerical modeling of the thrombosis. At this stage, the model is made of two parts. The first one is the simulation of the blood flow itself and the other one is the modeling of the transport and the aggregation of the blood cells to form a thrombus. The blood flow in a living body is a rather complicated process because of the great amount of interaction between the blood and the vessel walls that can vary a lot depending on each individual, we assume here that the geometry is static (no fluid-structure interaction). Furthermore the vessel geometry is difficult to obtain with a great accuracy even with the most advanced imaging techniques, because of the typically small size of the blood vessels and the difficulty to distinguish the exact location of the vessel walls.

Nevertheless, once the geometry is obtained, the flow in blood vessels is a rather straightforward process to simulate, at a macroscopic scale. The main uncertainty is related with the boundary conditions to be applied at inlets/outlets. At this stage, simple uniform boundary conditions are used, but time dependent boundary conditions will be added to reproduce physiological conditions.

The blood cells transport and the thrombosis processes are much more complicated and are not yet well understood and many details are still actively investigated. Here, our goal is to propose a simplified model that will use a limited amount of parameters but which will nevertheless be able to reproduce the basic dynamics of a thrombus formation, at large scale. In particular the model should be able to detect if a thrombosis is possible or not in a patient specific aneurysm, if the placement of a stent should be done and how it may be designed to optimize the thrombosis formation.

In what follows, we describe the basics of the particle transport and thrombosis formation models. The blood flow is of course an important part of the simulation but it is not discussed here as its simulation is well understood. All our numerical models have been developed using the Lattice Boltzmann (LB) and the multiparticle cellular automata (CA) method (see for instance [3]). Moreover, all the implementations discussed hereafter are done within the open-source parallel library Palabos [21].

2.1.1 The Palabos software

The Palabos library is an open-source highly efficient parallel library based on the lattice Boltzmann method[3, 24]. It has been developed for years, partly at the University of Geneva, and is proven to simulate accurately flow in complex geometries. Thus it can be used for patient specific blood flow simulations. In particular, a comparison between the commercial software CFX and Palabos has been made and a very good match between the solvers has been found (see <http://www.palabos.org/academia/usecases/30-cfxbench>, and Fig. 1).

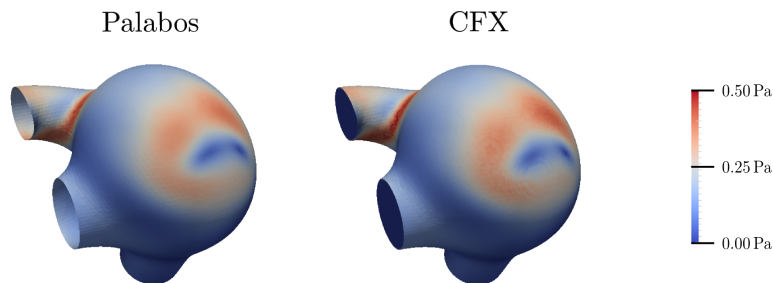


Figure 1: Comparison of the wall shear stress between Palabos and the commercial software CFX.

Furthermore the fact that the lattice Boltzmann method does not require any complicated mesh generation allows a very fast grid generation even for the most complicated geometries and the time spent for this tedious problem is negligible when compared to the characteristic time of a simulation. As an illustration, fig. 2 shows the streamlines produced by the presence of a stent in an aneurysms. This stent is not a flow diverter, but it shows the possibility to include the explicit strut geometry in the Palabos software.

Simulations with flow diverter will be reported in a next deliverable.

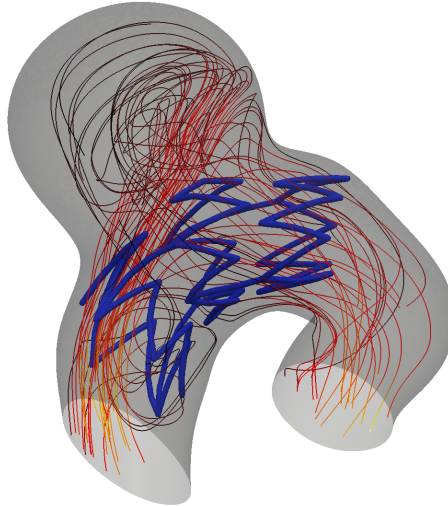


Figure 2: Simulation of the flow in a stented aneurysms, from a geometry and stent deployment provided by subcontractor StrokeLab.

Finally, a very good parallel efficiency has been found even on very large parallel computers, such as the Blue Gene/P (see Fig. 3).

2.1.2 Particle transport model

The blood cells are transported by an underlying flow which is simulated thanks to a lattice Boltzmann algorithm. In Fig. 4 one can see an example of an aneurysm geometry and the norm of the velocity after convergence of the flow with a constant velocity imposed at the inlet.

Two different models have been implemented so far for the transport of particles. In each of them the particles are considered as passive scalars. Although the macroscopic equation that they are representing is the same process (an advection-diffusion equation) there are major differences in their nature and therefore in their numerical efficiency.

The first consists of a multiparticle cellular automaton (CA) based on discrete particles while the second is based on a lattice Boltzmann model.

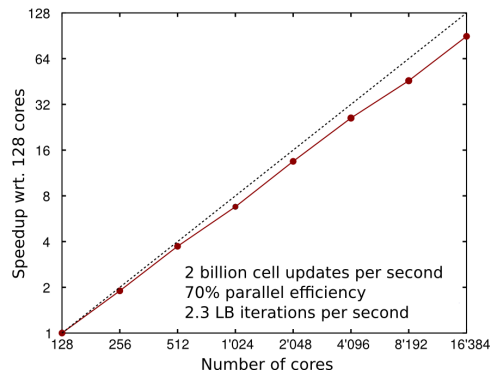


Figure 3: Speedup of an aneurysm simulation performed on the CADMOS Bluegene/P. An efficiency of about 70% is obtained in the “strong” scaling case and on a span of two orders of magnitude in the number of processors.

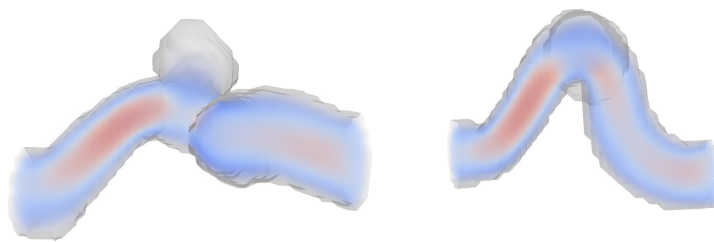


Figure 4: The velocity norm in an aneurysm geometry from different angles (red for high velocity and blue for low).

2.1.3 The discrete particle method

This particles transport algorithm follows the approach presented in [17, 26]. The particles are located on a mesh which is coincident with the grid used for the fluid. On the particles mesh q discrete microscopic velocities $\{c_i\}_{i=0}^{q-1}$ are defined, which connect each grid point with its $q - 1$ neighbors ($c_0 = 0$). Here we use the so-called D3Q19 lattice [24]. In order to advect the particles, the velocity field $u(x, t)$ is computed at grid point x and at time t from the fluid flow solver. Then the following algorithm is used (see Fig. 5)

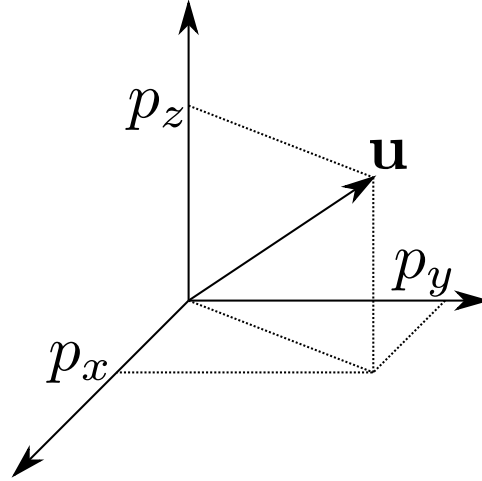


Figure 5: Velocity and probabilities of being streamed along one principal axis. The overall probability of being advected along a vector c_i is made of the probabilities of being advected or not advected in each one of these principal axes.

1. The octant, \mathcal{O} , where u lies is selected.
2. A projection of the velocity on the principal axes of the selected octant is performed, and each projection is defined as the probability of a particle to be advected along the axis. These probabilities are labeled p_x, p_y, p_z respectively.
3. A subset of the microscopic $c_{i \in \mathcal{O}}$ is defined, where

$$c_{i \in \mathcal{O}} = \{c_i | c_i \in \mathcal{O}\}. \quad (1)$$

Or equivalently all the c_i s that are in \mathcal{O} .

4. The probability $P(c_{i \in \mathcal{O}})$ of being advected along a microscopic velocity $c_{i \in \mathcal{O}}$ is computed thanks to a composition of the probabilities of being advected with probabilities p_x, p_y and p_z or not advected with probabilities $(1 - p_x), (1 - p_y), (1 - p_z)$. For example, $c_{i \in \mathcal{O}} = (1, -1, 0)$ the corresponding probability is given by $P((1, -1, 0)) = p_x p_y (1 - p_z)$.
5. The N particles are propagated along each direction $i \in \mathcal{O}$ by

$$N_{i \in \mathcal{O}} = NP(c_{i \in \mathcal{O}}). \quad (2)$$

Since $P(c_{i \in \mathcal{O}})$ is usually a real number, the value of $N_{i \in \mathcal{O}}$ is truncated to the lowest integer. The remaining particles obtaining by this truncation are added to N_0 (the particles with zero velocity).

In the original model this advection step was done by using a completely probabilistic manner [17]. Here we assume that there are enough particles per grid point to allow a deterministic advection of particles for numerical efficiency reasons.

2.1.4 Boundary conditions

Since this model is a pure advection model (it contains only a small numerical diffusivity), one of its main issues lies in the regions where the fluid has zero velocity. When the particles are transported to such places they are trapped and cannot leave, since there is almost no diffusion due to this numerical scheme. These places act like sinks where particles tend to accumulate in a non-physical way. Furthermore more practical problems arise, when trying to compute mean-values for the evaluation of the convergence (or not) of the numerical scheme.

If not treated in the appropriate fashion the no-slip boundary conditions are perfect candidates for such “sink effects” since they have by definition zero flow velocity. Here we decided to reuse the well known cellular idea of “bounce-back” to forbid accumulation of particles in near-wall regions. At each time step on all boundary nodes the incoming particles are simply send back from where they came, using a reflexion

$$N_{\text{opp}(i)}^{\text{out}} = N_i^{\text{in}} \quad (3)$$

and then are streamed along the i -th direction, where $\text{opp}(i)$ stands for the opposite of the i -th direction, where $\mathbf{c}_i = -\mathbf{c}_{\text{opp}(i)}$. This boundary condition conserves the particle number by construction and imposes a zero momentum.

2.1.5 The lattice Boltzmann advection-diffusion method

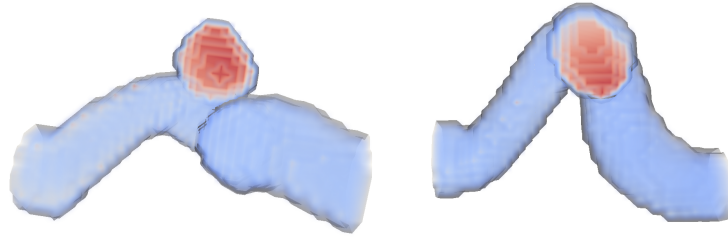


Figure 6: Particle concentration (red for high concentration, blue for low) in the aneurysm viewed from two different axes when using the LB advection diffusion algorithm.

The advection-diffusion algorithm method using the lattice Boltzmann method (see [8]), is presented here. Again a discrete lattice is used, but unlike the kind of the cellular automaton model, the lattice used here can be restricted to a D3Q7 lattice, thus reducing the memory need of a complete simulation by roughly 25%. The algorithm is following the standard LB approach of passive scalars (with density ρ) advected by a fluid velocity \mathbf{u}

$$f_i(\mathbf{x} + \mathbf{c}_i, t + 1) = f_i(\mathbf{x}, t) - \frac{1}{\tau} \left(f_i(\mathbf{x}, t) - f_i^{(\text{eq})}(\mathbf{x}, t) \right), \quad (4)$$

where

$$f_i^{(\text{eq})} = w_i \rho \left(1 + \frac{\mathbf{c}_i \cdot \mathbf{u}}{c_s^2} \right), \quad (5)$$

with c_s the sound speed of the lattice, w_i the lattice weights, and τ the relaxation time, related to the diffusivity, κ , of the scalar field by the relation

$$\kappa = c_s^2 (\tau - 1/2). \quad (6)$$

The simulation result is illustrated in Fig. 6.

2.1.6 Boundary conditions

The boundary conditions on no-slip walls used in the LB advection-diffusion case must simply enforce the absence of mass flux through the vessel walls. This is again achieved through bounce-back. It can be shown by using the Chapman–Enskog expansion that this boundary condition naturally enforces a no-mass flux condition through the vessel wall.

2.1.7 Advantages and drawbacks of each model

The main advantage of the particles model is its unconditional stability and its reasonable accuracy, even at low resolution. In addition, an extra diffusion can be easily added if needed to avoid the spurious particles accumulation near the wall.

However, in the present problem, the spatio-temporal resolution is dictated by the blood flow and it is sufficiently fine to avoid the stability and accuracy problems present in the LB advection-diffusion model. Therefore, the increase of computing performance and the saving of memory makes the LB approach more promising for our large scale, 3D simulations.

Another potential advantage of the lattice Boltzmann advection-diffusion model in the present application concerns the possibility of applying off-lattice boundary conditions and thus increase the accuracy of the model (the bounce-back boundary condition is only first order accurate, while off-lattice boundary condition approaches are second order). Nevertheless, this approach would require to modify the thrombosis model to be compatible with this more accurate approach.

2.1.8 Thrombosis formation model

The thrombosis model can be applied without any major modification to the CA (discrete particle) or LB approaches. Since in the CA case one deals with a number of particles per site and in the LBM case with a density of particles per site, only a simple renormalization of the number of particles is needed to switch from one model to the other.

The thrombosis is modeled here as the process for a certain amount of particles described in the preceding section to adhere and aggregate altogether to a wall, making them part of this wall, on which other particles may

then adhere, thus building up the thrombus. This growth process modifies the geometry of the computational domain and therefore modifies the flow pattern.

To implement this process in our model, the following rule is defined: with probability p_a , a fluid cell becomes a wall cell provided that the conditions below are satisfied.

1. The fluid cell is next to a wall.
2. The number N of particles on this node is bigger than a critical number N_c .
3. The wall shear stress w_{ss} is smaller than a critical threshold value, w_c .
4. Conditions 1-3 are satisfied for a time bigger than a critical time t_c .

Alternatively conditions 3 and 4 can be replaced by a continuous probability $p_a(w_{ss})$ that will have a shape similar to the one presented in Fig. 7. The critical time t_c is taken into account by the increase value of the cumulated adhesion probability p_a over consecutive time iterations. In the future, the

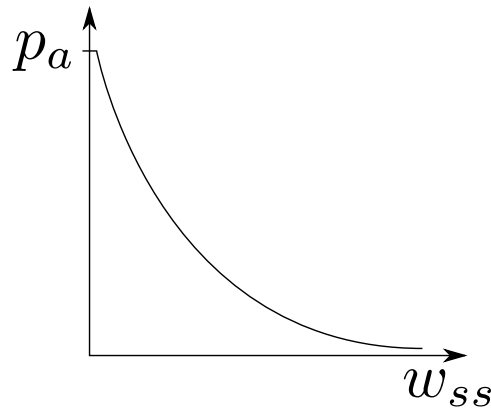


Figure 7: Probability of adhesion p_a with respect to the wall shear stress w_{ss} . The higher the w_{ss} the lower the probability of adhesion.

value of these parameters need to be extracted and validated from the biological experiments performed in WP2 and the clinical observation from WP3.

2.1.9 Simulation

As an example of a thrombus formation using this transport-thrombosis model, along with a fluid flow simulation, using the lattice Boltzmann method, a simulation in a real aneurysm geometry is performed (see Fig. 8).

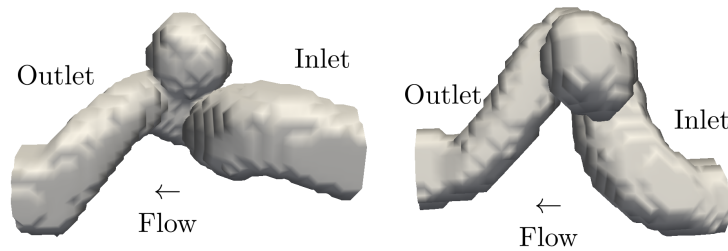


Figure 8: A patient specific geometry (with two different view angles) of the aneurysm used in this section to illustrate the macroscopic numerical model of thrombosis.

Before describing qualitatively the results a few more approximations are performed, mainly for efficiency reasons. While the spatial scales of the fluid and of the particles are of the same order of magnitude (between micro-meter and centimeter) and are therefore comparable, the thrombosis formation is a much slower process than the time scale necessary for the flow to adapt to the modifying geometry (see Fig.9). The first one is of the order of weeks to months while the latter is of the order of a second. Therefore, one can use a decoupled multiscale approach to model these two processes. First, the flow is simulated until a steady state is reached (at this stage pulsatile flows are not considered). Then the flow simulation is stopped and only the velocity field obtained is used for the particles transport and the thrombosis process modeling. Then if at least one fluid node is transformed into a wall node (thrombosis), the particles simulation is stopped and stored and the flow is again simulated with the new geometry. These processes are iterated until the geometry of the flow is not changed anymore. For pulsatile flow, another multiscale strategy might be more appropriate. This will be discussed in the next deliverable.

The parameters of the simulation are chosen as shown in Table 1. These values are adequate to produce a thrombus in the model but are not yet

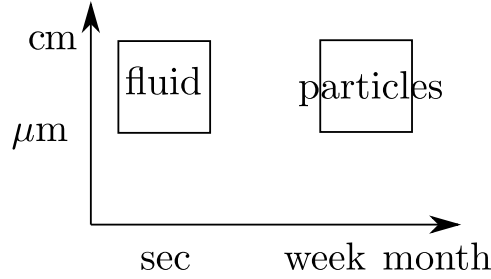


Figure 9: The scale separation map of the particles (and thrombus) and of the fluid flow. One can see that while the spatial scales are similar the temporal scales differ of many orders of magnitude.

biologically validated. The boundary conditions are a “plug” flow at inlet

N_c	w_c	t_c	p_a
50	$2.5 \cdot 10^{-5}$	50	0.5

Table 1: The parameters chosen for the spontaneous thrombosis present in this section, in lattice units.

and a zero velocity gradient at the outlet. The flow is therefore steady, and the Reynolds number is chosen to be of $Re = UL/\nu = 10$ ($U \sim 10^{-2}[m/s]$, $L \sim 10^{-3}m$, $\nu \sim 10^{-6}[m^2/s]$). For the simulation we chose the following parameters in lattice units: $L = 20$ (vessel diameter) and $U = 0.05$, thus giving $\nu = 0.1$. The simulation therefore is made of approximately 10^5 computational nodes.

A crucial part of the simulation consists in a proper initialization of the particle distribution. It can be easily understood that if one starts with an uniform distribution over the whole computational domain, which could be in particular bigger than N_c will lead to dramatically different results than when the initial distribution is obtained by actually transporting the particles from the inlet of the flow. Here we chose to initialize the particles density to zero everywhere and to apply a constant distribution of particles at the inlet. The outlet boundary condition is to have a zero particles density gradient in the direction normal to the outlet.

2.1.10 Cellular automaton transport model

The simulation carried out in this subsection is performed with the cellular automaton transport algorithm for the particles.

As can be seen from Fig. 10 a thrombosis is spontaneously forming. With the parameters chosen, one can see that while the aneurysm is being clotted, and the flow in the parent vessel is being disconnected from the aneurysm and therefore the blood cells cannot anymore be streamed in it, a part of the aneurysm remains unclotted. This unrealistic effect is a con-

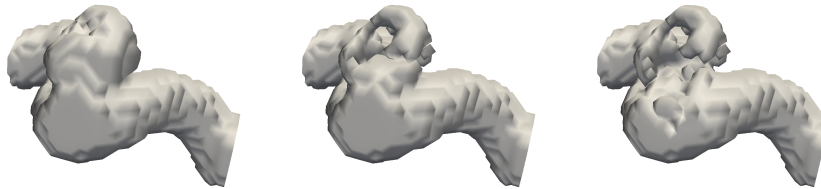


Figure 10: The time evolution of the wall of the blood vessel (from left to right). As can be seen the aneurysm is disappearing with time. It can be noticed, that a part of the aneurysm lumen does not disappear completely, but is detached from the parents vessel. This unrealistic effect is a consequence of a too small diffusivity of the platelets.

sequence of the absence of diffusion of the transported particle in the CA advection model, which may lead to disconnected flow regions which do not contain enough particles ($N < N_c$) for the thrombosis to occur.

The above simulation results were obtained in about three hours on a desktop computer with two cores.

2.1.11 LB Advection-diffusion model

From Fig. 11 one can see that other geometry of the thrombus are obtained with the LB transport model, although the adhesion and growth parameters are used as in the CA case.

The reason of the different behavior is that in the LB case the diffusivity of particles is much bigger than in the CA case. Here we chose the diffusivity to be a hundred times smaller than the viscosity, or a Prandtl number of $Pr = \nu/\kappa = 100$, or in lattice units $\kappa = 0.001$ (in real blood the diffusivity of platelets is found to be of the order of $\kappa \sim 10^{-9}[m^2/s]$). Although, this

value is smaller than in real fluids, it has been chosen for numerical stability reasons (for $Pr = 1000$ and the diffusivity corresponding to platelets in blood, the code was unstable). This value is obviously much bigger than in the numerical diffusion of the cellular automaton case. As one can notice,

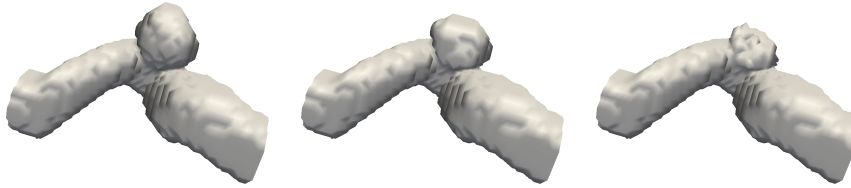


Figure 11: The time evolution of the wall of the blood vessel (from left to right). As can be seen the aneurysm is being occluded as time goes on.

in this case the thrombosis has a more uniform shape when compared with the cellular automaton transport model (see Fig. 10).

These simulations were obtained in about two hours on a desktop computer with two cores.

The above simulations have been performed at a rather low resolution (10^5 fluid nodes) in order to save computing resources. Fig. 12 shows, for the sake of illustration, a simulation with a higher spatial resolution (about 2×10^6 fluid nodes and an increased temporal resolution). The computing time is around 4 hours on 50 cores.

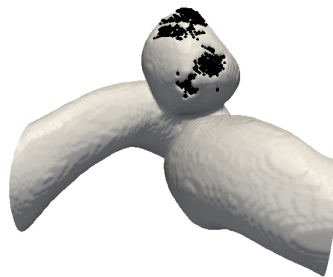


Figure 12: Illustration of the thrombus formation (black region) in a high resolution simulation.

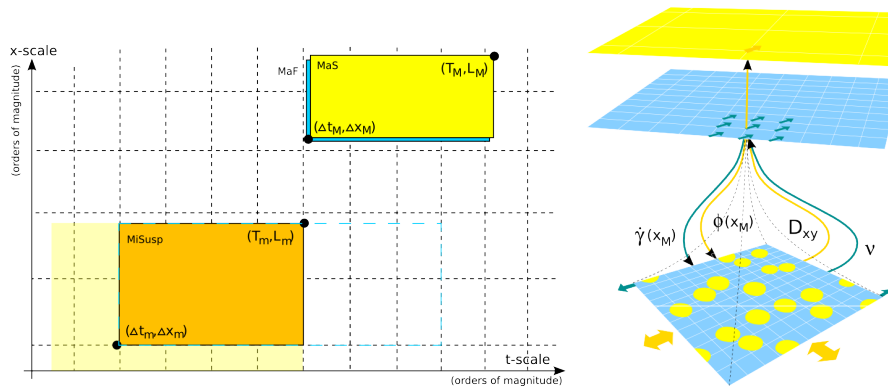


Figure 13: HMM coupling between a macroscopic and a microscopic solver of the dynamics of a simple complex fluid (a monodisperse hard-sphere suspension here). Left: Scale Separation Map illustrating the separation of microscopic and macroscopic processes. Right: On the macroscale solvers for the dynamics of the fluid and the solid phase span the whole domain but don't resolve the spatiotemporal details of the fluid's constituents. On each lattice node of the macroscopic solvers a microscale solver can be invoked to obtain transport properties and viscosities for given boundary conditions defined by macroscopic shear-rate and fluid/solid volume ratio.

2.2 The microscopic numerical model

2.2.1 Hierarchical model of blood flow

If spatiotemporal scales of the processes on the cell level and the dynamics of blood flow on the macroscopic level are well separated, a micro-macro modeling approach can be considered. The CxA formalism [11] provides templates for the coupling of such two models and in case both models describe processes in the same physical domain the multiscale models falls into the class of the Heterogeneous Multiscale Method (HMM) [27]. In that, a microscopic fully-resolved representation of blood and its constituents can be coupled to the macroscopic solver with a significant reduction of the computational problem without introducing significant errors. The use of HMM for complex fluids has been demonstrated [16] with the application to the simulation of monodisperse hard-sphere suspensions. The idea is illustrated in figure 13.

In such an approach the macroscopic solver spans the whole geometry while the microscopic solver holds, in several spatially separated instances,

only a limited part of the domain, just large enough to resolve spatial correlation of the constituents on the microscale. And the microscale model only has to run for a temporal extent sufficient to resolve temporal correlations of micro-structures. However, this approach is only valid if the two scales can clearly be separated, i.e., spatiotemporal resolution of the macroscale solver is (much) larger as the spatiotemporal extend of the microscopic system. The smallest spatial scale is given by the dimensions of the stent struts and the inter-strut distance. The first, depending on the type of strut, is in the order of $10\ \mu\text{m}$, the second in the order of $100\ \mu\text{m}$. An RBC is in the order of $8\ \mu\text{m}$, that means that around the struts an HMM approach is not justified. Here, a grid-refinement approach is more suitable where the space around the struts is fully resolved and couples, at its boundaries, to another model for the bulk, e.g., using the described HMM approach.

One of the technical challenge of an application of HMM to our problem is the modeling of microdomains representing a piece of the endothelium boundary together with the blood flow along it. Here, classic Lees-Edwards bcs can not be applied because there is no periodic extension of the microdomain in direction of the bulk. The in/outflow of fluid and particles into the microdomain will have to be created artificially. A couple of ideas how to realize this exist, however, this is work in progress.

The coupling between micro and macromodel and the measurements at both levels would have to be extended by a number of quantities. For a simple hard-sphere suspension shear rate, particle density, viscosity, and diffusion tensor was sufficient. However, for a multicomponent flow as blood diffusivities for each particle type will have to be measured and passed to the macromodel which has to be able to handle the advection and diffusion of each of these particle types.

The micromodel will be extended, first by a simple adhesion model, later by the implementation of an aggregation and coagulation model for the cell-based biochemical processes. The coagulation model deals with quantities that show microdynamics but that have also to be transported over macroscopic distances, e.g. those describing the biochemical state of platelets. Many quantites might have to be considered. The definition of the microscale adhesion and coagulation dynamics, and how these quantities couple to the macroscopic flow and transport model described in 2.1 is work in progress.

Though the use of HMM reduces the computational costs significantly, the actual execution of the simulation on HPC facilities stays mandatory. For the parallelization of the macro- and/or micromodel a number of question arise. The discussion and implementation of this is work in progress.

2.2.2 Preliminary Model of RBCs and Platelets Suspended in Flow

A microscale model of blood flow and its extensions through integrated models for the adhesion, aggregation, and coagulation, on the cell level serves several purposes.

First, such a model will be used to validate the assumptions in the macro-model regarding the rheology of blood and its platelet-transport properties. Such a validation can be carried out in two possible ways: one in which the micromodel is run in a small Lees-Edwards simulation box in which a shear is imposed on the blood model and, resembling a viscometer, viscosities and shear-induced diffusivities of the platelets can be obtained over a physiological range of shear rates. The values for these quantities and their variance can then be used to be compared with the assumptions of a constant viscosity and a constant isotropic diffusivity of the platelets in the macromodel. Another way to provide validation is to run both, macro and micromodel, in a sample geometry with the same inlet/outlet conditions after which flow profiles, platelet density distribution, and platelet trajectories could be compared. In blood, RBCs have a significant impact on viscosity and platelet transport. If the agreement of the prediction from both models do not agree sufficiently the macromodel might have to be revised in order to provide a better match.

Once macroscopic rheology and transport have been validated, the future microscopic adhesion model can be used to validate the assumptions on the platelet sticking probability $p(WSS, \dots)$ in the macromodel. This, again, could be carried out in a viscometer setting or a fully resolved sample geometry. The next step would then be to provide a way to validate the assumptions on the effect of coagulation and aggregation of platelets, expressed in the parameters N_c and T_c . Again, this can be done through simulations resembling a Couette-type of viscometer, or in a fully resolved sample geometry.

Of course, the micromodel has to be validated as well. The rheology of

blood and transport properties of platelets is a well studied field and sufficient information in the literature exist to carry out the validation of the mechanical properties of the micromodel without additional in-vitro or in-vivo experiments. The close collaboration with WP2 allows us to validate the assumptions that will be made on the initial adhesion of platelets through a comparison with the results from the Impact-R experiments in which different plate coatings can be used. The results from the flow chamber experiments will allow us then to validate our assumptions on coagulation and aggregation properties through the evaluation of the time-resolved growth of thrombus in an artificial aneurysm geometry that will be reproduced in a simulation.

In the following, a preliminary mechanical model is introduced. In the next deliverable (D4.2) the work in progress on the model for adhesion, aggregation and coagulation will be presented.

Following a literature research on approaches to the modeling of fully-resolved blood, i.e., including explicit representations of RBCs and platelets, we investigated two possible approaches in detail:

In one approach we coined **CeBa (Cells made of Balls)**, and which is similar to the model presented in [19], cells are represented by one (platelet) or a chain of 10 spheres (RBC). This approach is a compromise between cells represented by a single geometrical object and the fully resolved finite-element representation of a cell membrane. This model can reproduce almost all modes of deformation of an RBC. However, like the single-object approach, it suffers from the neglect of any further mechanical properties like the membrane's ability to rotate around the viscous (not visco-elastic) plasma. This property is leading to tank-treading dynamics that has substantial impact on the rheology [14] and transport properties of blood [5]. In flow through small vessels or constriction this model cannot reproduce the shapes RBCs assume there and other rheological aspects of the flow [19]. Also, using this approach, there would be a number of technical challenges, e.g. the coupling of extended objects to a Lattice-Boltzmann-based fluid solver. Special numerical methods would have to be developed and validated.

The other approach we have coined **SuMO (Suspensions of Membraneous Objects)**. To be able to capture all important aspects of rheology and transport properties of blood as well as active biochemical processes on

the cell surface, we decided for a modeling approach that describes blood cells as explicitly resolved flexible membranes by means of a finite-element (FE) model. RBCs and platelets consist of a multiple-layer membrane and a viscous inner fluid whose viscosity is similar to that of the plasma. A treatment of blood cells in this way is therefore reasonable. It is the most realistic representation of the membrane mechanics, also allowing to reproduce tank-treading. This approach has been shown to reproduce the dynamics of RBCs and the whole blood with good accuracy. The different cell types differ in the stiffness of the membrane: RBCs are rather flexible whereas platelets do not change their spherical shape much (shape changes due to activation will not be considered). Stiffness, bending and stretching properties can be directly tuned by numerical parameters in the model. These flexible membranes are coupled to the LBM fluid using the immersed boundary method [20]. The model constitutes an improvement over existing similar approaches in the literature (see for example [19, 15]) in several aspects of the accuracy of the hydrodynamic interaction of membranes and the fluid. For example, surface-curvature dependent corrections to the lubrication force have been implemented, and corrections have been implemented in order to ensure conservation of the inner volume. Another advantage of the FE membrane approach is, that with the point-wise representation of the membrane objects exist to which additional dynamics can be assigned rather straightforwardly. This plays an important role for the implementation of the coagulation model that is under development (see deliverable D4.2, M18).

A preliminary 2D implementation of this model has been realized and, in order to validate it, applied to simple stylized problems. We are still in the process of validating the model and tuning the various mechanical parameters. Parallel to this, we are working on a 3D implementation of the SuMO model that will allow us then to carry out the validating comparisons with in-vitro experiments.

2.2.3 Simulations

We have simulated the flow of whole blood in 2D through the stylized aneurysm geometries presented in [10] and carried out preliminary studies of the influence of suspended particles on the flow and transport proper-

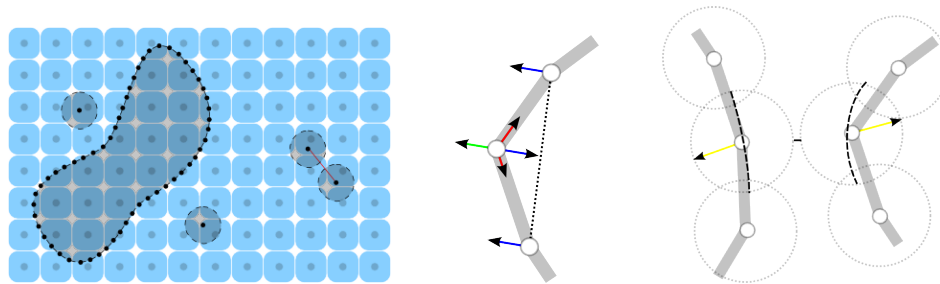


Figure 14: Left: In the SuMO model RBC's and platelets are represented by an FE model of the membrane. Coupling to the fluid is realized using the immersed boundary method applied at the membrane points. Middle: The mechanical model consists of points that are connected by spring-and-damper elements between neighboring membrane points to realize stretch and compression of surface elements (red), spring-and-damper elements between next-nearest membrane points to represent membrane bending forces (blue), and normal forces are applied in order to conserve the internal volume (green). Right: A curvature dependent lubrication correction is applied between membrane points of different cells to capture the hydrodynamical interaction between membranes realistically.

ties. In these simulations we tried to input the basic properties of blood suspensions that are important in thrombosis, erythrocytes and platelets with a varying range of hematocrit values on different Reynold numbers. This model was presented as a proof of concept rather than a full blown 2D simulation of blood and the objective was to understand a qualitative behavior of the deformable suspended particles in more complex geometries and by no means producing quantitative results.

The suspended particles used were of two types, deformable particles with a constant Volume to Surface ratio, representing the RBCs, and hard sphere particles representing the platelets. These particles were simulated in aneurysm geometries with two different neck-to-diameter aspect ratio (1.0 and 0.5), stented and not. The results revealed that the transport properties of the particles are highly dependent on the the applied stent, the Reynolds number of the flow and the hematocrit.

The influx of particles into the aneurysm from the main channel was considerably reduced when a stent was applied, with a lower porosity stent yielding more reduction in the influx. A relatively high Reynolds number (~ 100) in combination with a low hematocrit ($\sim 20\%$) made the dispersion

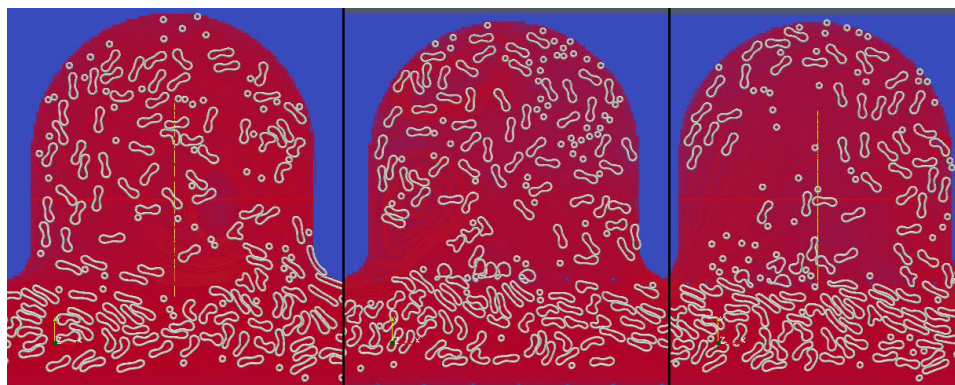


Figure 15: Snapshot of the simulations, without stent and stented with high and low porosity

of the particles and the influx to almost disappear for our given aneurysm geometries. This behavior can find its explanation in the FåhræusLindqvist effect [7], in which the erythrocytes move over the center of the vessel, leaving plasma at the wall of the vessel.

A 2D simulation would need almost 1 million particles (RBCs and platelets) to reach a hematocrit of 40% in a 4 mm artery. For this reason a turn to the HPC infrastructure with the proper modifications in an algorithmic and implementation level are mandatory.

2.3 Multiscale description of thrombosis

This section presents the first steps towards a multiscale description of the thrombosis in cerebral aneurysm. The final model will be discussed in deliverable D4.2.

At first a literature research on the medical basics of clot formation has been performed. This provides a deeper insight of all medical and biological processes which occur during clot formation. In Subsection 2.3.1 the results are described.

After this a coupling scheme has been defined, which includes all the results from the biological processes. This scheme gives a first idea of the kind of data that has to be exchanged between the different parts of a multiscale simulation. The results are presented in subsection 2.3.2.

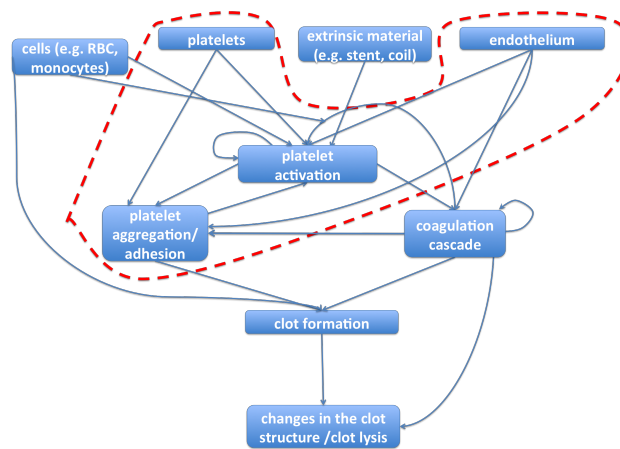


Figure 16: The Biological Processes

2.3.1 The Biological Processes

In this subsection the major biological processes and their interactions which lead to the formation of a blood clot are presented.

The two major key parts of clot formation are

- platelet activation and aggregation
- coagulation cascade.

Platelets in their inactive form have a discoid shape with a smooth rippled surface [23] with an average diameter of $1.5 - 2 \mu\text{m}$ [12]. They have a various number of receptors on their surface which can be stimulated by various pro- and anticoagulant agents. In addition the platelets organelles include different kinds of granules. These granules host a various number of adhesive proteins, plasma proteins and growth factors (e.g. factor V, van-Willebrand Factor (vWF))[9]. Additionally platelets have receptors on their surface which support their ability to aggregate to the wall, exogenous surfaces and to each other. Platelet activation can be triggered by

- exposure to high shear stresses (approx. 5 Pa [1, 22])
- extrinsic materials (e.g. stent, coil) [2, 12]
- collagen XII release from injured endothelium [13, 25]
- activated platelets
- coagulation factors [12]

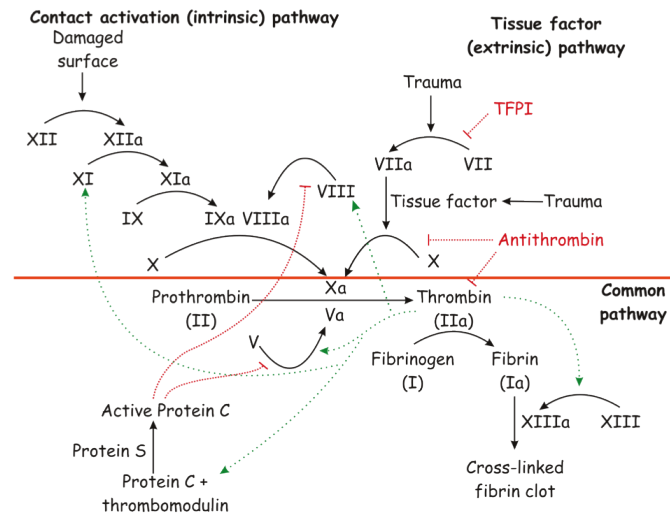


Figure 17: The Coagulation Cascade

Activated platelets change their shape from discoid to spherical [12] and start to expose proteins and growth factors stored in their granules. They also start forming aggregates and attach to the subendothelial matrix at an injured vessel wall.

The second key for clot formation is the coagulation cascade which leads to the production of fibrin from its inactive form fibrinogen. Fibrin aggregates to fibrin strands which in the latter forms a cross linked mesh. In this mesh cells from the blood, e.g. RBCs, are caught and incorporated.

The coagulation cascade (see Figure 17) consists of two major pathways (extrinsic and intrinsic) which lead to a common pathway in the end. Among a various number of proteins, e.g. Protein C and S, and agents e.g. vWF the twelve coagulation factors I-XIII (factor VI is not defined) are the major contributors to the cross-linked fibrin mesh. Besides fibrin thrombin and its inactivated form prothrombin plays an important role in coagulation. It is the central link of the two pathways and activates fibrinogen to fibrin [1].

2.3.2 The Coupling Scheme

In this subsection the coupling between the different parts of the SSM is presented in detail. The idea is to get an overview of what has to be done by the different 'agents' and how one could set up a communication structure (see figure 18). It is also a good way of finding the accurate way of

simplifying the simulation so that it can be run in finite time on a suitable HPC system.

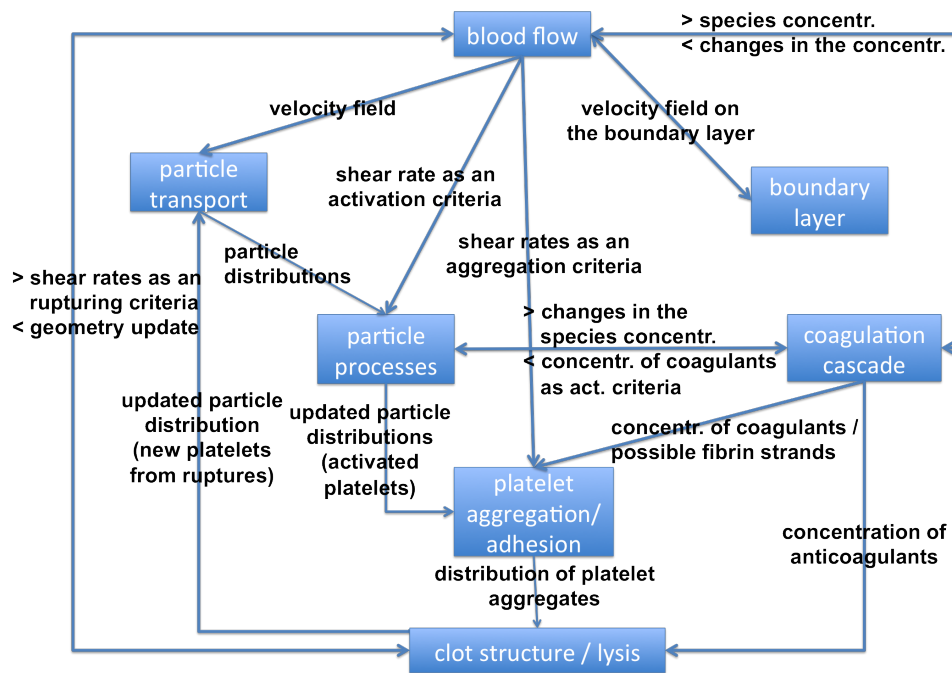


Figure 18: The Coupling Scheme

3 Conclusions

As explained in the above sections, the result obtained in WP4 after 12 months are in agreement with the DoW, and we are confident that we will keep progressing along the line of the proposal.

At this stage, our macroscopic model shows the expected qualitative behavior, as compared to the behavior of the 2D model proposed in [18, 4] and the general clinical observations. However, this model still need some tuning, in particular for better boundary conditions and, more importantly, for implementing the time-dependent flow. As discuss above, this might requires a different multiscale strategy to deal with the very different time scale of the flow and the thrombus grow. At this stage, we conclude that the CPU time to simulate the thrombus evolution on a patient specific geometry is perfectly acceptable (order of the hour on a two-core laptop) knowing the excellent scalability of the LB approach on large parallel computers.

For a quantitative analysis of the model a validation against biological and clinical data is obviously crucial. In particular the relevance and values of the parameters described in section 2.1.8 (or alternatively the probability curve of Fig. 7) must be carefully discussed. This is a important task for the rest of this project. A preliminary statistical analysis of the experiment conducted in WP2 (impact-R results) suggests that parameters such as the probability of adhesion can indeed be extracted and used to calibrate our macroscopic model.

In order to progress in this direction, we plan to develop a simulation of the experimental device used in WP2 (Impact-R), both with the microscopic and the macroscopic numerical models. With this, we expect to assess the validity of assumptions made for each level of description. This work will be reported in detail in a future deliverable.

It should be noted that the analysis of the experimental results is a task that was underestimated in the DoW and that will probably require a reallocation of resources within the WP4.

Of course, clinical observations will complete the development of the macroscopic numerical model. First it will offer the ultimate way to validate the model for large temporal and spatial scales and its ability to predict the evolution of a real case. Secondly, it will provide a way to calibrate/define some parts of the model that cannot be derived from the microscopic level.

For instance the microscopic process that is responsible for the interruption of the thrombus growth is still an open question in the literature. It seems clearly related to the value of the shear rate. If no first principle biological mechanism can be identified, an empirical value can be extracted only from the clinical follow up of patients.

There exists another open question that must be discussed in the next steps of this project. It is related to the transport of blood particles. So far we have used a simple advection-diffusion for passive scalars, with constant diffusion coefficient. The microscopic model for suspension shows that the transport properties are more complicated when the shape of the particles are taken into account. In particular, the distribution of the particle is not homogeneous. Therefore a coarse graining of the microscopic simulation in simplified geometries, but with the right amount of RBC and platelets will be performed to evaluate the possibility to use the passive scalar assumption in the macroscopic model. Another way to validate the assumptions on rheology and platelet transport is to carry out parameter studies in a rheometer-like simulation setup. This type of simulation could then also be used to validate additional adhesion interaction in the micro-model against the Impact-R experiments.

As far as model validation is concerned, an additional approach can be proposed, based on recent observations made at the Hospital of Geneva [6]. Time-dependent angiography images of several patients reveals a stagnation of the flow in the deeper part of the aneurysm. This stagnation zone changes significantly when measure just before and just after stenting. On the one hand, the size and shape of this area provides a simple way to validate the quality of the stent deployment in the simulation. On the other hand, it has been suggested in [6] that the variation of the stagnation zone before and after stenting gives a good indicator of the growth of a thrombus in the aneurysm. Being able to explain such an observation as an emergent property of our model would offer a very convincing validation.

References

- [1] M. Anand, K. Rajagopal, and K.-R-Rajagopal. A model for the formation and lysis of blood clots. *Pathophysiology of Haemostasis and Thrombosis*, 34(2-3):109–120, 2005.
- [2] M. Anand, K. Rajagopal, and K.R. Rajagopal. A model incorporating some of the mechanical and biochemical factors underlying clot formation and dissolution in flowing blood. *Journal of Theoretical Medicine*, 5(3–4):183–218, 2003.
- [3] B. Chopard and M. Droz. *Cellular Automata Modeling of Physical Systems*. Cambridge University Press, 1998.
- [4] B. Chopard, R. Ouared, D. A. Ruefenacht, and H. Yilmaz. Lattice boltzmann modeling of thrombosis in giant aneurysms. *Int. J. Mod. Phys. C*, 18:712–721, 2007.
- [5] Lindsay M. Crowl and Aaron L. Fogelson. Computational model of whole blood exhibiting lateral platelet motion induced by red blood cells. *International Journal for Numerical Methods in Biomedical Engineering*, 26(3-4):471–487, March 2010.
- [6] O. Bonnefous et al. A novel method for the assessment of the intra-aneurysmal flow changes induced by flow diverter stents using motion estimation based upon dsa images. *American Journal of Neuroradiology (AJNR)*, 2011. Submitted.
- [7] Robin Fåhræus and Torsten Lindqvist. The viscosity of the blood in narrow capillary tubes. *American Journal of Physiology – Legacy Content*, 96(3):562–568, March 1931.
- [8] Z. Guo, B. Shi, and C. Zheng. A coupled lattice BGK model for the Boussinesq equations. *Int. J. Num. Meth. Fluids*, 39:325–342, 2002.
- [9] P Harrison and E Martin Cramer. Platelet -granules. *Blood reviews*, 7:52–62, 1993.
- [10] Miki Hirabayashi, Makoto Ohta, Daniel Rüfenacht, and Bastien Chopard. Lattice boltzmann analysis of the flow reduction mechanism in stented cerebral aneurysms for the endovascular treatment

- computational science ICCS 2003. In Peter Slood, David Abramson, Alexander Bogdanov, Jack Dongarra, Albert Zomaya, and Yuriy Gorbachev, editors, *Computational Science ICCS 2003*, volume 2657 of *Lecture Notes in Computer Science*, chapter 108, page 658. Springer Berlin / Heidelberg, Berlin, Heidelberg, June 2003.
- [11] A. G. Hoekstra, A. Caiazzo, E. Lorenz, J.-L. Falcone, and B. Chopard. Complex automata: multi-scale modeling with coupled cellular automata. In A. Hoekstra, J. Kroc, and P. Slood, editors, *Modeling complex systems with cellular automata*, volume chapter 3. Springer Verlag, 2010.
 - [12] S Kamath, AD Blann, and GYH Lip. Platelet activation: assessment and quantification. *European Heart Journal*, 22(17):1561–1571, 2001.
 - [13] Malgorzata M Kamocka, Jian Mu, Xiaomin Liu, Nan Chen, Amy Zollman, Barbara Sturonas-Brown, Kenneth Dunn, Zhiliang Xu, Danny Z Chen, Mark S Alber, and Elliot D Rosen. Two-photon intravital imaging of thrombus development. *Journal of Biomedical Optics*, 15:1–7, March 2010.
 - [14] T. Krüger. *Computer simulation study of collective phenomena in dense suspensions of red blood cells under shear*. PhD thesis, Ruhr-Universität Bochum, 2011.
 - [15] T. Krüger, F. Varnik, and D. Raabe. Efficient and accurate simulations of deformable particles immersed in a fluid using a combined immersed boundary lattice Boltzmann finite element method. *Comput. Math. Appl.*, 61(12):3485–3505, June 2011.
 - [16] E. Lorenz and A. G. Hoekstra. Heterogeneous Multiscale Simulations of Suspension Flow. *Multiscale Model. Sim.*, 9(4):1301+, 2011.
 - [17] A. Masselot and B. Chopard. A lattice boltzmann model for particle transport and deposition. *Europhys. Lett.*, 42:259–264, 1998.
 - [18] Rafik Ouared and Bastien Chopard. Lattice boltzmann simulations of blood flow: Non-newtonian rheology and clotting processes. *J. Stat. Phys.*, 121(1-2):209–221, 2005.

- [19] Wenxiao Pan, Dmitry A. Fedosov, Bruce Caswell, and George E. Karniadakis. Predicting dynamics and rheology of blood flow: A comparative study of multiscale and low-dimensional models of red blood cells. *Microvasc. Res.*, 82(2):163–170, September 2011.
- [20] Charles S. Peskin. Numerical analysis of blood flow in the heart. *J. Comput. Phys.*, 25(3):220–252, November 1977.
- [21] The Palabos project. <http://www.lbmmethod.org/palabos>.
- [22] J M Ramstack, L Zuckermann, and Mockros F L. Shear-induced activation of platelets. *J Biomechanics*, 12:113–125, 1979.
- [23] W Siess. Molecular mechanisms of platelet activation. *Physiological Reviews*, 69(1):58–178, January 1989.
- [24] S. Succi. *The lattice Boltzmann equation for fluid dynamics and beyond*. Oxford University Press, Oxford, 2001.
- [25] Oren Traub and Bradford C. Berk. Laminar shear stress: mechanisms by which endothelial cells transduce an atheroprotective force. *Arteriosclerosis, Thrombosis, and Vascular Biology*, 18:677–685, January 98.
- [26] K. Tsunematsu, B. Chopard, J.-L. Falcone, and C. Bonadonna. Comparison of two advection-diffusion methods for tephra transport in volcanic eruptions. *Commun. Comput. Phys.*, 9(5):1323–1334, 2011.
- [27] W. E, B. Engquist, X. Li, W. Ren, and E. Vanden-Eijnden. Heterogeneous Multiscale Methods: A Review. *Comm. Comp. Phys.*, 2(3):367+, 2007.